

Cd9 Protects Photoreceptors from Injury and Potentiates Edn2 Expression

Toshiro Iwagawa,¹ Yuko Aihara,¹ Daisy Umutoni,¹ Yukihiro Baba,¹ Akira Murakami,² Kenji Miyado,³ and Sumiko Watanabe¹

¹Division of Molecular and Developmental Biology, Institute of Medical Science, University of Tokyo, Tokyo, Japan

²Department of Ophthalmology, Graduate School of Medicine, Juntendo University, Tokyo, Japan

³Department of Reproductive Biology, National Research Institute for Child Health and Development, Setagaya, Tokyo, Japan

Correspondence: Sumiko Watanabe, Division of Molecular and Developmental Biology, Institute of Medical Science, The University of Tokyo, 4-6-1 Shirokanedai, Minato-ku, Tokyo 108-8639, Japan; sumiko@ims.u-tokyo.ac.jp.

Received: August 29, 2019

Accepted: January 5, 2020

Published: March 9, 2020

Citation: Iwagawa T, Aihara Y, Umutoni D, et al. Cd9 protects photoreceptors from injury and potentiates Edn2 expression. *Invest Ophthalmol Vis Sci.* 2020;61(3):7. <https://doi.org/10.1167/iovs.61.3.7>

PURPOSE. Cd9 is a tetraspanin membrane protein that plays various roles in tissue development and disease pathogenesis, especially in cancer, but the expression patterns and function of Cd9 in retinal development and disease are not well understood. We asked its roles during retinal photoreceptor degeneration by using CD9-knockout mice.

METHODS. Cd9 knockout mice and rd1 mice were used to examine roles of Cd9 for progression of photoreceptor degeneration. Reverse transcription-polymerase chain reaction and immunohistochemistry were mainly used as analytical methods.

RESULTS. Cd9 transcripts were only weakly expressed in retina at embryonic day 14, but its expression level subsequently increased and peaked at around postnatal day 12. In 6-week-old female mice derived retina, mRNA expression decreased slightly but was maintained at a significant level. Published RNA-sequencing data and immunohistochemistry indicated that Cd9 was expressed abundantly in Müller glia and weakly in other retinal neurons. Notably, when photoreceptors were damaged, Cd9 expression was increased in rod photoreceptors and decreased in Müller glia. Cd9 knockout mice retinas developed normally; however, once the retina suffered damage, degeneration of photoreceptors was more severe in Cd9 knockout retinas than control retinas. Induction of *Edn2*, which is known to protect against photoreceptor damage, was severely hampered. In addition, induction of *Socs3*, which is downstream of gp130 (Il6st), was weaker in Cd9 knockout retinas.

CONCLUSIONS. Taken together, these findings indicate that, although Cd9 was dispensable for normal gross morphological development, it protected rod photoreceptors and enhanced Edn2 expression, possibly through modulation of gp130 signaling.

Keywords: Cd9, photoreceptor, degeneration, Edn2

Cd9 encodes a tetraspanin membrane protein that was originally reported to be a motility-related factor based on the inhibition of migration caused by anti-Cd9 antibodies in multiple cancer cell lines.^{1,2} Subsequent studies revealed that Cd9 acted as a tumor suppressor³ as well as an oncogenic and pro-metastatic molecule.⁴ In addition, a contribution of Cd9 to tumor angiogenesis has been suggested,⁴ and because of the biological activities in cancer, Cd9 has attracted attention as a possible therapeutic target.^{4,5}

Various interacting molecules of Cd9 have been reported.⁶ For example, Cd9 associates with various integrins and modulates integrin signaling pathways, including those involving focal adhesion kinase, phosphoinositide 3-kinase, and p130Cas.^{6,7} Cd9 interacts with other members of the tetraspanin superfamily and consists of membrane domains, termed tetraspanin-enriched microdomains.⁸ Through such associations, Cd9 plays various roles in hematopoietic and endothelial cells.⁸

In the neural system, Cd9 has been well studied in glioma,^{9,10} but it is also expressed in normal specific cell

subsets in both the central and peripheral nervous systems, including glial lineage cells such as Schwann cells, as well as in oligodendrocytes and neurons.¹¹ Cd9 is also involved in neurite formation via an association with integrins.¹²

In adult bovine eye, *Cd9* transcripts are strongly expressed in the ciliary epithelium and cornea, but only weakly expressed in the neural retina.¹³ In humans, cultured retinal progenitor cells from postmortem premature infants express Cd9.¹⁴ Although Cd9 is a well-studied molecule, its detailed expression patterns and functions during retinal development have not been reported. We previously found that Cd9 was enriched in c-kit-positive late retinal progenitor cells, and an assessment of its functions by short hairpin RNA-mediated downregulation in retinal explant cultures suggested a role for Cd9 in Müller glia development.¹⁵ We therefore hypothesized roles for Cd9 in the differentiation and maintenance of the retina, which have not been previously investigated. In the present study, we examined the detailed expression patterns of Cd9 in degenerating retinas and found that Cd9 was downregulated in Müller glia, but

upregulated in photoreceptors during rod degeneration. We then assessed the detailed role of Cd9 in retinal degeneration by using the Cd9 knockout (Cd9-KO) mouse during retinal development and found that Cd9 played protective roles in photoreceptors, at least partially through cooperative signaling transduction of Il6st receptor signals leading to the expression of Edn2.

METHODS

Animals

All animal experiments were approved by the Animal Care Committee of the Institute of Medical Science, University of Tokyo, and conducted in accordance with the Guidelines laid down by the National Institutes of Health in the United States regarding the care and use of animals for experimental procedures and the Association for Research in Vision and Ophthalmology statement for the use of animals in ophthalmic and vision research. ICR mice were obtained from Japan SLC Co, and we confirmed that the mice were free of rd1 mutation. The day when a vaginal plug was observed was considered as embryonic day 0 (E0), and the day of birth was termed as postnatal day 0 (P0). Generation of Cd9-KO mouse and Cd9 and Cd81-double knockout (Cd9/Cd81-DKO) mouse was previously described.^{16,17} These mice were backcrossed into the C57BL/6J background. All mice were confirmed that the mice were free of rd1 and rd8 mutations. The rd1 (C3H/HeSlc) mouse was purchased from Japan SLC Co.

Analysis of MNU or NaIO₃ Administrated Mouse Retina

As photoreceptor and retinal pigmented epithelium (RPE) degeneration models, administration of N-Methyl-N-methyl urea (MNU) and NaIO₃ were used, respectively. MNU was administrated intraperitoneally at 120 mg/kg, and the eyes enucleated after indicated days, and retinas were isolated. NaIO₃ was administrated by tail vein injection at 120 mg/kg, and the eyes were enucleated after indicated days. Phosphate-buffered saline (PBS)-administrated mouse retinas were used as control. The isolated eyes were subjected to the immunohistochemistry, or fluorescence activated cell sorting (FACS).

FACS

Retinas were isolated from enucleated eyes, incubated with 0.25% Trypsin for 15 minutes. Then, retinas were treated with 20% fetal bovine serum and DNaseI, dissociated into single cells and stained with PE conjugated anti-Cd73 antibody (BD Pharmingen) for 30 minutes on ice. Retinas were washed with 2% bovine serum albumin and stained with propidium iodide. Cd73 negative and positive cells were collected using FACSaria II (BD).

RT-qPCR

Total RNA was purified from the mouse retina using Sepasol RNA I Super G (nacalai tesque), and complementary DNA was synthesized using ReverTra Ace qPCR RT Master Mix (TOYOBO). Quantitative polymerase chain reaction (qPCR) was performed using the SYBR Green-based method (THUNDERBIRD SYBR qPCR Mix, TOYOBO), using

the Roche Light Cycler 96 (Roche Diagnostics). The data were normalized by using Gapdh and Sdha, which were used as an internal control, following the way previously described.¹⁸ Sequences of the primers are as follows; Gapdh: 5'- ttagaagcaaacctgtccagcttc -3', 5'- cataccaggaaatgagcttgac -3', Sdha: 5'- gtgtgaagtagggcaggtcc -3', 5'- acaaggcactggctcgatac -3', Cd9: 5'- tggggctatacccacaagga -3', 5'- gctttgagt-gtttcccgtg -3', Nr2e3: 5'- gaaacacgaggcctgaagga -3', 5'- gggagcaggaggagcaattt -3', Rho: 5'- ggcccccaattttatgtgcc -3', 5'- tagtactcggctgctcgaa -3', Edn2: 5'- ttctgccatgaagactg -3', 5'- atggcctttctgtcacctc -3', Fgf2: 5'- cccacacgtcaactacaac -3', 5'- actggagtatttccgtgacc -3', Lif: 5'- aaacggcctgcatctaagg -3', 5'- agcagcagtaaggcacaat -3', Socs3: 5'- caaggccggagatttcgctt -3', 5'- gggaacttctgtgtgggtga -3', Stat3: 5'- cagttcctggcacttg-gat -3', 5'- gactcttcgaggaatcggc -3'.

Immunohistochemistry

Immunostaining of frozen sections was done as described previously.¹⁹ Briefly, retinas were enucleated and fixed with 4% paraformaldehyde for 20 minutes or 1 hour at room temperature, treated with 15% sucrose overnight, treated with 30% sucrose for 6 hours, embedded in OCT compound (Leica), and sectioned (10 μm thickness) using the cryostat (Leica, CM3050S). Primary antibodies used are mouse monoclonal antibodies anti-Glutamine synthetase (Chemicon), photoreceptor-specific nuclear receptor (PNR; ppmx), HuC/D (Molecular Probes), Ccnd3 (Cell Signaling), rabbit polyclonal antibodies anti-Calbindin 28k (Chemicon), Pax6 (BioLegend), sheep polyclonal antibody anti-Chx10 (Alpha Biologicals), and rat monoclonal antibody anti-Cd9 (Santa Cruz Biotechnology). Signals of primary antibodies were visualized using appropriate secondary antibodies conjugated with Alexa 488 or Alexa 594 (Molecular Probes). To measure the thickness of inner nuclear layer (INL) and outer nuclear layer (ONL), the central area, close to the optic nerve head, in more than three sections of each sample was analyzed. The thickness at three different parts was measured in each section, and the average was calculated. The average of all samples in each experimental group was calculated and unpaired two-tailed *t* test was used to evaluate statistical significance.

TUNEL Assay

DNA fragments resulting from the apoptotic activation of intracellular endonucleases were detected in retinal sections by incorporation of fluorescein labeled dUTP using the In Situ Apoptosis Detection Kit #MK500 by TAKARA BIO INC, as described by the manufacturer. Briefly, sections were washed with PBS and the endogenous peroxidase was inactivated using methanol (containing 0.3% H₂O₂) at room temperature for 20 minutes. Sections were washed three times with PBS and permeabilized with permeabilization buffer for 5 minutes on ice. After washing three times with PBS, sections were incubated with the TUNEL reaction mixture (consisting of terminal deoxynucleotidyl-transferase enzyme and labeling safe buffer) for 90 minutes in a 37°C humidified incubator. The labeling reaction was terminated by washing three times with PBS. Sections were incubated with Anti-FITC HRP Conjugate at 37°C for 30 minutes and washed with PBS 3 times for 5 minutes each time. After coloring with DAB at room temperature for 10 minutes, the reaction was terminated by washing with distilled water. Nuclear was stained with DAPI. Apoptotic

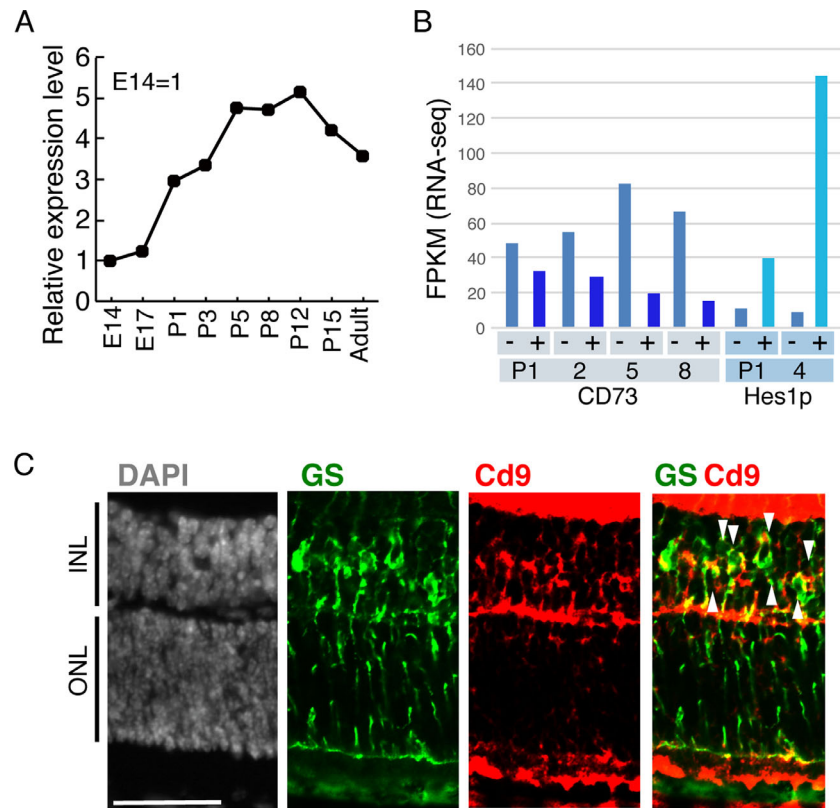


FIGURE 1. Transition of the expression of Cd9 during retinal development. **(A)** Transition of expression levels of *Cd9* transcripts during retinal development. Whole retinas at indicated developmental stage were harvested, and RT-qPCR was done using a primer specific for *Cd9*. The values were normalized to Cq value of *Gapdh* and *Sdha*, and expressed as relative to E14 value. An 8-week-old mouse was analyzed as an adult mouse. **(B)** Expression levels of *Cd9* transcripts in subpopulations of developing retina. Fragments per kilobase of exon per million mapped fragments (FPKM) value of RNA-seq data of purified Cd73 positive rod photoreceptors and Cd73 negative other cells at P1, 2, 5, 8 (GEO: GSE71462), and Hes1-promoter positive Müller glia and negative other cells at P1 and P4 (GEO: GSE86199) are shown. **(C)** Immunohistochemistry using anti-Cd9 and -GS, which marks Müller glia, antibodies in a P10 mouse retinal frozen section. One representative sample out of samples from three independent mice was shown. Nuclei were visualized by staining with DAPI (gray). Arrowheads indicate GS and Cd9 double positive cells. Scale bar: 50 μ m.

cells were observed using Axio Imager M1 (Zeiss) fluorescent microscope. To count TUNEL-positive cells, the central area, close to the optic nerve head, in more than three sections of each sample was analyzed. The number of TUNEL-positive cells in 100 μ m retina at three different parts was counted in each section, and the average was calculated. The average of all samples in each experimental group was calculated and unpaired two-tailed *t* test was used to evaluate statistical significance.

Statistics

When more than two conditions were compared, Tukey's test was performed. When two conditions were tested, Student *t*-test with two tails was performed. A *P* value was considered significant if less than 0.05. All data, except for Figure 1A, were obtained from more than three independent mice.

RESULTS

Expression Patterns of Cd9 During Retinal Development

We previously examined the expression of *Cd9* transcripts during retinal development and found that the mRNA

expression of *Cd9* was low in retinas at E14, but constantly increased until P12.¹⁵ We first confirmed and examined in greater detail the transition in expressions of *Cd9* transcripts during retinal development by reverse transcription (RT)-qPCR of mouse whole retinas. *Cd9* expression increased constantly during retinal development and peaked at P12; it then decreased, but significant expression levels were maintained until the adult (8 weeks) stage (Fig. 1A). *Cd9* has been previously reported to be expressed in glial cells in the brain.²⁰ We also previously showed that *Cd9* was enriched in c-kit-positive late retinal progenitor cells and Müller glia cells.¹⁵ We characterized in more detail the types of retinal cells expressing *Cd9* transcripts by using rod photoreceptors and other retinal cell type-specific RNA sequencing (GSE71464), which was previously conducted in our laboratory.²¹ At P1 and P2, *Cd9* was expressed at slightly lower levels in Cd73-positive rod photoreceptors than in the Cd73-negative fraction, which consisted of retinal cells except for rod photoreceptors (Fig. 1B). At P5 and P8, *Cd9* was expressed in much higher levels in the Cd73-negative fraction than in Cd73-positive cells (Fig. 1B), suggesting that retinal cells other than rod photoreceptors were the major cell types expressing *Cd9* transcripts. We next examined the expression of *Cd9* transcripts in developing Müller glia by using our previously published RNA-sequencing

(GSE86199) data of retinas from *Hes1* promoter-driven EGFP (*Hes1p*-EGFP)-expressing mice.^{22,23} *Cd9* was expressed at higher levels in the *Hes1p*-EGFP-positive Müller glia cell fraction at P1, and the difference was much greater at P4, because the expression levels of *Cd9* in the *Hes1p*-EGFP-positive fractions largely increased, but the expressions in the *Hes1p*-EGFP-negative fractions remained weak (Fig. 1B). Taken together, the results confirmed that *Cd9* was mainly expressed in Müller glia in developing retina.

We next examined the spatial expression pattern of the *Cd9* protein by immunostaining using frozen sections of the mouse retina at P10. We found that the signals of *Cd9* mostly overlapped with GS, which is a marker of Müller glia (Fig. 1C, arrowheads), supporting the idea that *Cd9* was almost exclusively expressed in Müller glia cells.

Retinal Morphological Development of Cd9-KO Mice Was Indistinguishable from that of Normal Mice

To clarify the roles of *Cd9* in retinal development, we next examined the retina of *Cd9*-KO mice.¹⁶ The frozen adult (8 weeks) *Cd9*-KO retinas were sectioned, and retinal development was examined by immunohistochemistry using antibodies against retinal subtypes. The thicknesses of the INL and ONL were indistinguishable between adult control and *Cd9*-KO retinas (Figs. 2A and B). We have previously shown that sh-RNA mediated *Cd9* knock-down in retinal explant cultures, resulting in failure of appropriate morphological development and a reduced number of GS-positive Müller glia.¹⁵ However, immunostaining using anti-GS antibody, which marks Müller glia, showed development of Müller glia in *Cd9*-KO retinas comparable to that in control retinas (Fig. 2C). To examine the difference of phenotypes caused by *in vivo* conditions and explant cultures, we cultured *Cd9*-KO mouse-derived retinas as explants; however, the gross morphological differentiation of Müller glia in this culture seemed indistinguishable from the control (data not shown). Currently, we cannot explain the contradiction, but genetic compensation of *Cd9* in *Cd9*-KO retina may be a possible mechanism. Immunostaining with Calbindin (horizontal cells), HuC/D (amacrine and retinal ganglion cells), *Isl1* (bipolar cells), *Brn3b* (retinal ganglion cells), *Ccnd3* (Müller glia), and *Rho* (rhodopsin) showed that all of these retinal subtypes developed normally (Fig. 2D), and the populations of these subsets of cells were also appropriate (data not shown) in *Cd9*-KO retinas.

Among the tetraspanin membrane proteins, *Cd81* has significant sequence homology with *Cd9*²⁴ and often plays redundant roles with *Cd9*.⁷ *Cd81* plays pivotal roles in cell-cell fusion, such as in sperm-egg²⁵ and muscle cell fusion,²⁶ and negatively regulates both HIV-induced cell fusion²⁷ and macrophage fusion.²⁸ We characterized the expression pattern of the *Cd81* transcript during retinal development by using the RNA-sequencing data, which was published by us (GSE71464, GSE86199),^{21,23} and found that *Cd81* was broadly expressed in retinal subtypes such as rod cells, Müller glia, and other cells (Fig. 3A). The expression levels of the *Cd81* transcript were high and relatively constant during retinal development, suggesting the possibility that *Cd81* functionally compensated for *Cd9* in *Cd9*-KO retinas. We next examined development of retinas from *Cd9* and *Cd81* double-KO (*Cd9/Cd81*-DKO) mice.¹⁷ The thicknesses of the INL and ONL were the same between the

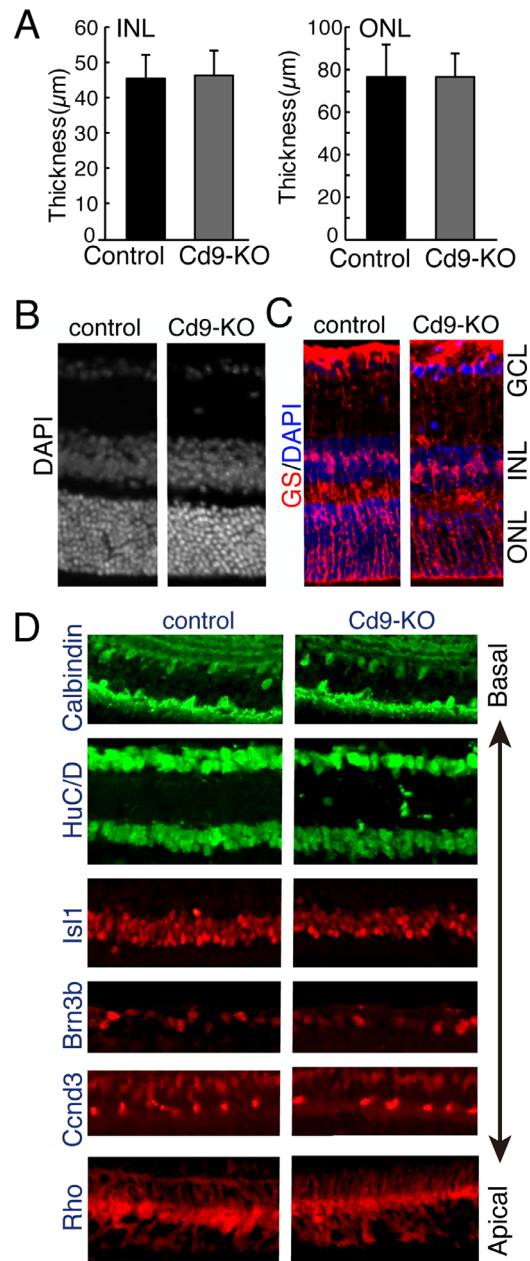


FIGURE 2. The retina develops appropriately in *Cd9*-KO mouse. (A) The thickness of INL and ONL of the retinas of adult control or *Cd9*-KO mice at 8 weeks was measured in frozen sectioned retina. The values are average of more than 9 sections from 3 mice for each genotype with standard deviation. (B–D) Immunohistochemistry by using indicated antibodies of frozen sections of the retinas of control or *Cd9*-KO mice was performed. All panels are shown as ONL to the bottom. The antibodies label specific subsets of retinal cells; GS (Müller glia), Calbindin (subsets of amacrine and horizontal), HuC/D (amacrine and RGC), *Isl1* (bipolar), *Brn3b* (RGC), *Ccnd3* (Müller glia), *Rho* (rod photoreceptor). Nuclei were visualized by staining with DAPI in B (gray) and C (blue).

control and *Cd9/Cd81*-DKO retinas (Fig. 3B). Immunohistochemistry of retinal subtype markers showed that bipolar cells (*Chx10*), horizontal cells (Calbindin), amacrine cells (HuC/D and *Pax6*), Müller glia (*Ccnd3*), rod photoreceptors (*Rho*), and cone photoreceptors (*M*-opsin) developed normally (Fig. 3C). These results indicated that *Cd9* and *Cd81*

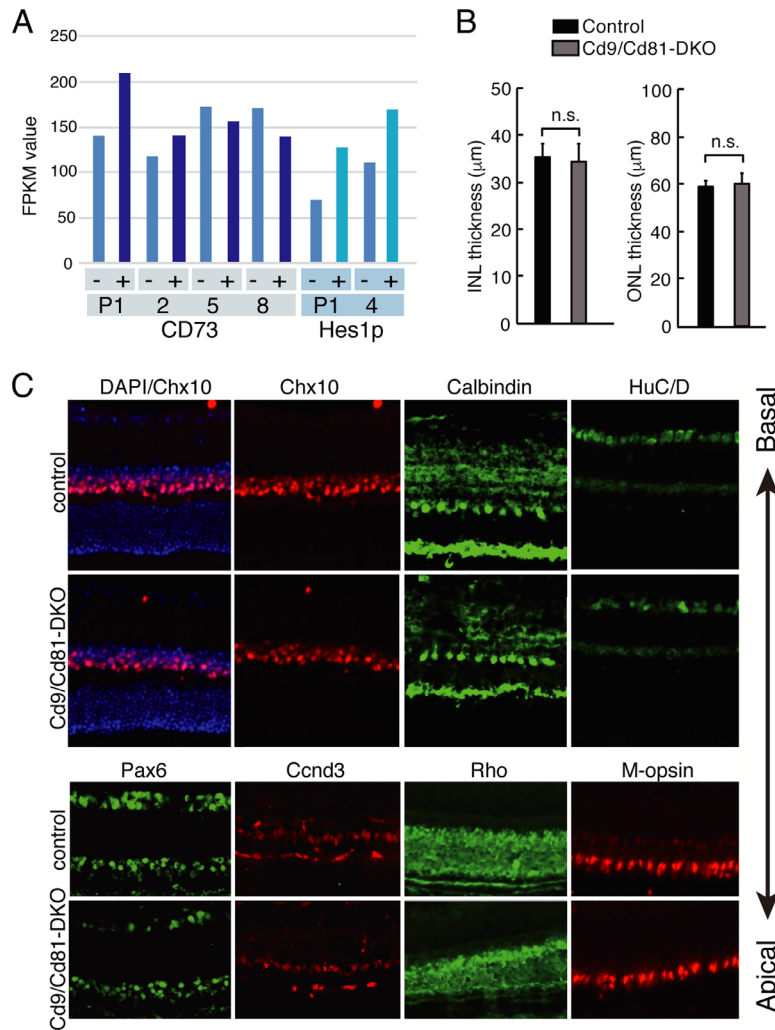


FIGURE 3. The retinas of Cd9 and Cd81 double knockout mice (Cd9/Cd81-DKO) showed comparable morphological development as in control retina. **(A)** Expression levels of *Cd81* transcript in developing retina. FPKM values of *Cd81* from RNA-seq of Cd73-positive rod photoreceptors and Cd73-negative other cells at P1, 2, 5, 8, and Hes1-promoter (Hes1p)-positive Müller glia and -negative other cells at P1 and P4 are shown. **(B)** Thickness of INL and ONL of retinas of adult (8 weeks) littermate control or Cd9/Cd81-double knockout mice (Cd9/Cd81-DKO) was examined in frozen sections. Values are average of 3 mice with standard deviation. Statistical analysis was done using Student *t* test with two tails. **(C)** Immunohistochemistry was done using frozen sections of Cd9/Cd81-DKO and control retinas with antibodies anti-Chx10 (bipolar), Calbindin (horizontal), HuC/D (amacrine and RGC), Pax6 (amacrine), Ccnd3 (Müller glia), Rho (rod), and M-opsin (cone). Nuclei were visualized with DAPI.

were dispensable for gross morphological development of the retina.

Photoreceptor Degeneration Induced the Expression of Cd9 in Photoreceptors

A previous study reported that *Cd9* was one of the upregulated genes after scraping of rat retinas.²⁹ We then determined whether the expression of *Cd9* transcripts in the pathogenic retina was altered. MNU and NaIO₃ are reagents known to induce degeneration of the rod and RPE, respectively, when they are administrated to mice.^{30–33} MNU or NaIO₃ was administrated to ICR mice as described in the Materials and Methods, and the retinas were harvested at 5 or 7 days after injection. RT-qPCR was then used to detect *Cd9* transcripts in whole retinas. The expressions of

Cd9 transcripts were augmented in retinas from both MNU- (Fig. 4A) or NaIO₃-treated mice (Fig. 4B), and the difference was statistically significant except for the NaIO₃ treatment at day 7 (Figs. 4A and B).

To determine whether upregulation of *Cd9* transcripts occurred in different retinal cell types, we purified retinal cells to obtain Cd73-positive rod photoreceptors and Cd73-negative cells using a cell sorter. We first examined purity of Cd73-positive and Cd73-negative cell fractions by examining the expression of rod photoreceptor specific gene *Nr2e3* by RT-qPCR. The expression of *Nr2e3* were enriched 17 times (control for NaIO₃ sample) to more than 170 times (NaIO₃-treated samples), suggesting that separation of photoreceptor and other cells were successfully performed (Supplementary Figure S1). The expressions of *Cd9* transcripts in the Cd73-positive rods were upregulated, and those in the Cd73-negative fraction were rather suppressed

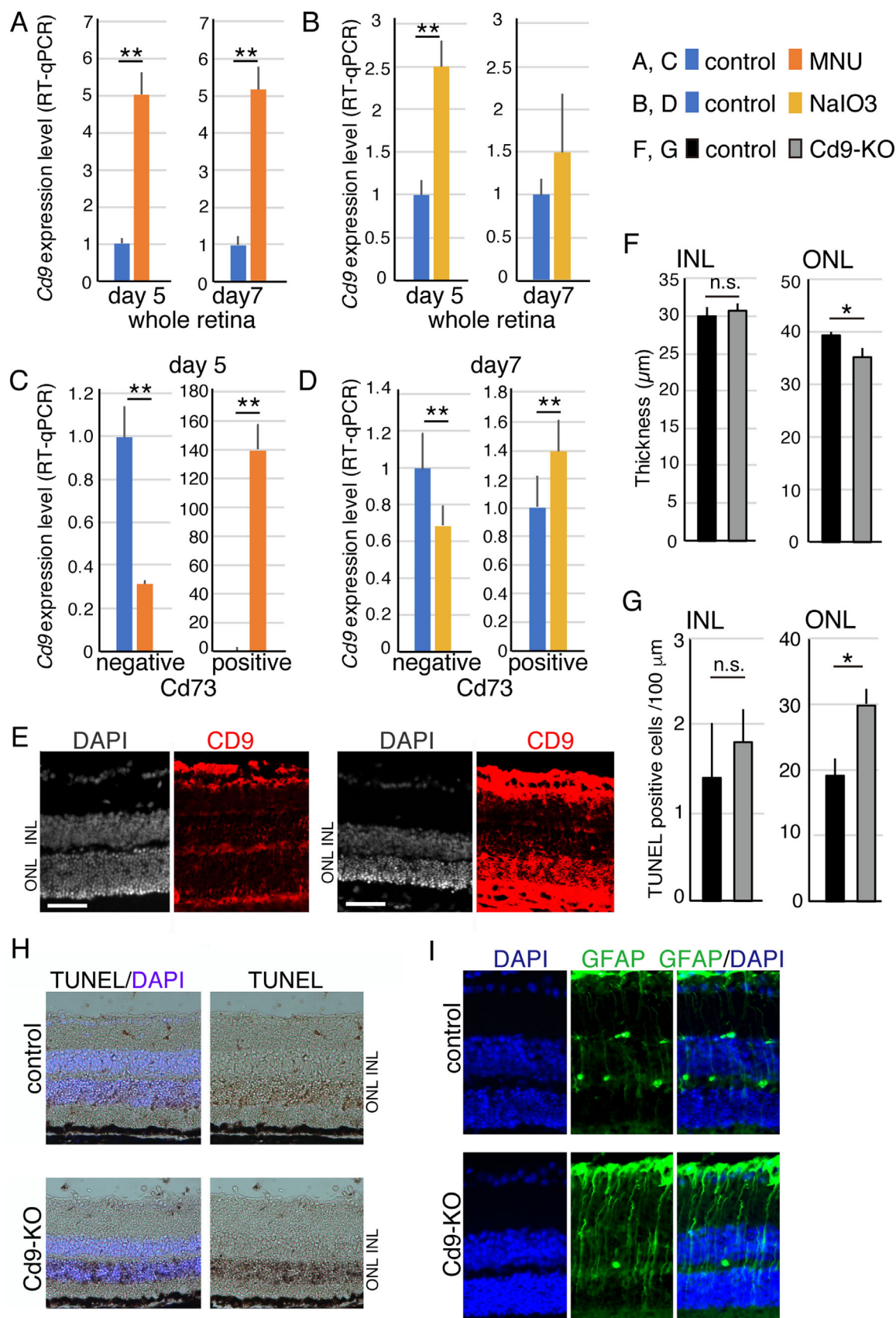


FIGURE 4. Augmentation of *Cd9* expression in MNU or NaIO3 induced retinal degeneration models. RT-qPCR to detect *Cd9* transcripts using total RNA prepared from whole retinas of (A) MNU or (B) NaIO3 induced retinal degeneration models. RT-qPCR of *Cd9* of purified Cd73 positive rod photoreceptors or Cd73 negative other retinal cells from mouse administrated with (C) MNU or (D) NaIO3. The mice were

treated with MNU or NaIO₃, then the retinas were harvested after 5 or 7 days, respectively. The retinal cells were fractionated to Cd73 positive and negative cell populations, and RT-qPCR to detect *Cd9* transcripts was done. The data are average value of 6 independent mice-derived samples with standard deviation. The number of mice used in these experiments are; control (6) and MNU-treated (6) mice for (A) and (C), and control (6) and NaIO₃-treated (6) mice for (B) and (D). (E) Immunohistochemistry of control and MNU-treated retina was done with Cd9 antibody. Nuclei was visualized with DAPI staining. MNU-induced photoreceptor degeneration in Cd9-KO retina was deteriorated. (F) Control littermates or Cd9-KO mice at 8 weeks were treated with MNU for 5 days. Thickness of INL or ONL of retinas derived from littermates or Cd9-KO mice was examined. (G) Apoptotic cells of the retinas were examined by TUNEL staining, and number of TUNEL-positive cells. (H) Staining pattern of TUNEL of control or Cd9-KO mice-derived retinal sections. Nuclei were visualized with DAPI staining, and the photos were taken by Nomarski imaging microscopy. (I) Immunohistochemistry of the retinal sections of littermates or Cd9-KO mice at 8 weeks with antibody against GFAP. Nuclei were visualized with DAPI staining. Scale bar: 50 μm.

(Figs. 4C and D). Because Müller glia is the only cell type that expressed Cd9 in normal retina, it is probable that *Cd9* expression in Müller glia was suppressed in degenerating retina. Immunohistochemistry with anti-CD9 antibody confers the augmented expression of CD9 protein in ONL (Fig. 4E).

Cd9-KO Retina Showed More Severe Degeneration Induced by MNU Administration than Did Control Mice-Derived Retina

Because upregulation of *Cd9* in photoreceptors has commonly been observed in both MNU- and NaIO₃-induced photoreceptor degeneration models, we determined the biological mechanism of this phenomenon. MNU was injected into control or Cd9-KO mice, and after 5 days, the retinas were harvested, frozen, and sectioned. The thickness of the INL was comparable between retinas derived from control and Cd9-KO mice, but the ONLs of the Cd9-KO retinas were thinner than those of control retinas (Fig. 4F). Furthermore, TUNEL analysis showed that apoptosis was more active in Cd9-KO retinas than in control retinas (Figs. 4G and H), suggesting that photoreceptors in the Cd9-KO retinas were more susceptible to MNU toxicity. We then examined the expression of glial fibrillary acidic protein (GFAP), a marker of activated Müller glia. The results showed stronger signals in Cd9-KO retinas than in control retinas (Fig. 4I).

We then determined whether these Cd9 processes in degenerating photoreceptors were also present in model systems. The rd1 mouse, a naturally occurring rod photoreceptor degeneration model,³⁴ has a mutation in the *Pde6b* gene. Cd9-KO and rd1 mice were crossed to obtain double homozygous mice (Cd9-KO;rd1). At P10, which corresponds to the stage before onset of degeneration of photoreceptors in rd1 mice, both the INL and ONL of the retinas of rd1 or Cd9-KO;rd1 mice showed comparable thicknesses (Figs. 5A and C). However, a thinner ONL in the Cd9-KO;rd1 mouse retinas than in rd1 mouse retinas was observed at P16 (Figs. 5B and D). In contrast, the INL was comparable between the rd1 and Cd9-KO;rd1 retinas (Figs. 5B and D). PNR is expressed specifically in rod photoreceptors,³⁵ and in much lower numbers in PNR-positive cells at P16 (Figs. 5E, H), which confirmed the greater reduction of rod photoreceptors in the retina of Cd9-KO;rd1 mice than in rd1 mice-derived retinas. We also examined the levels of *Nr2e3* and *Rbo* transcripts, both of which were expressed in a photoreceptor-specific manner. Both levels were severely suppressed in Cd9-KO;rd1 mice at P16 (Figs. 5F, G), supporting the idea that loss of photoreceptors was induced more in Cd9-KO;rd1 retinas than in control rd1 retinas. Taken together, the results showed that loss of Cd9 in rd1 mice did not affect the devel-

opment of retinas, but once photoreceptor degeneration started, loss of Cd9 resulted in more severe photoreceptor degeneration.

Activation of Müller Glia and Microglia May not be Perturbed in Retinal Degeneration of Cd9-KO;rd1 Mice

Müller glia and microglia are activated when photoreceptor degeneration occurs, so we examined these possible activations in Cd9-KO;rd1 retinas. Müller glia activation was examined by GFAP expression patterns, and microglia activation using an antibody to Iba1. At P10, no activation of microglia or Müller glia was observed, but both signals were observed at P16 (Fig. 5I). However, the signal intensity and number of cells were similar between retinas derived from rd1 and Cd9-KO;rd1 mice, suggesting that the activation of Müller glia and microglia was not perturbed by the absence of Cd9, at least at P16 in rd1 mice. Because we observed stronger GFAP signals in MNU-treated retinas (Fig. 4H), we carefully examined P10 retinas, and found that GFAP expression was occasionally observed in both rd1- and Cd9-KO;rd1-derived retinas, but we did not observe a definite difference between the two types (data not shown).

The Expression of Cytokines Induced by Photoreceptor Degeneration Was Perturbed in Cd9-KO;rd1 Retinas

To identify the molecular mechanism of action, we used RT-qPCR to characterize the expression of cytokine transcripts, which were induced by and involved in photoreceptor degeneration. The cDNA was first prepared from whole retinas of rd1 and Cd9-KO;rd1 mice at P10 and P16. The *Lif* gene is known to be transcriptionally activated in Müller glia when photoreceptor degeneration occurs.³⁶ As expected, the expression levels of *Lif* transcripts were slightly induced at P10 in rd1 mice retinas (Fig. 6A), and the levels in retinas derived from Cd9-KO;rd1 mice were slightly lower than that in rd1 mice retinas (Fig. 6A).

At P16, the level of *Lif* in rd1 retinas was increased, and the level in Cd9-KO;rd1 retinas was the same as that of rd1 mice (Fig. 6B). *Fgf2* and *Edn2* are known to be induced in damaged photoreceptors,³⁷ and the expression of the *Fgf2* transcript was strongly induced in rd1 mice retinas at P10 (Fig. 6A). This induction was also observed in Cd9-KO;rd1 retinas, and the difference was not statistically significant at P10 (Fig. 6A). *Edn2* was strongly induced in rd1 retinas at P10 and P16, and the level of *Edn2* in Cd9-KO;rd1 retinas was much lower in both stage (Figs. 6A, B). *Lif* is known to induce *Edn2* and *Fgf2*, and although severe suppression of *Edn2* expression was observed, the expression level of *Lif*

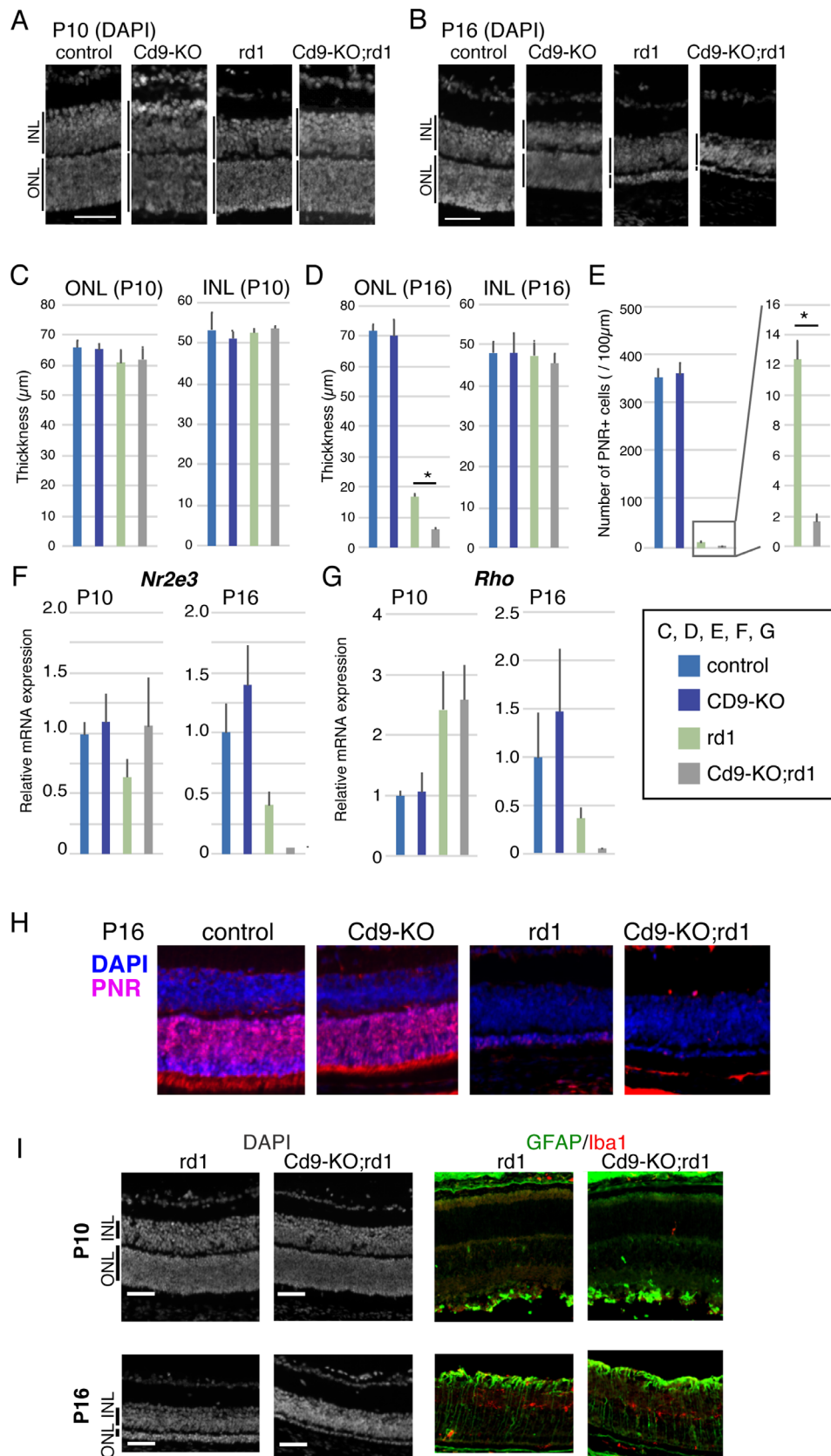


FIGURE 5. Knockout of Cd9 deteriorates photoreceptor degeneration in rd1 mice. Sections of control, Cd9-KO, rd1, or Cd9-KO;rd1 retinas at (A) P10 and (B) P16 were stained with DAPI to visualize the nuclei. (C, D) Thickness of ONL and INL of the retinas was measured in frozen sections stained with DAPI, and average of more than 9 sections of 3 independent mice derived retinas with standard deviation. *Scale bars:* 50 μ m (A, B). (E) Immunohistochemistry of the retinas at P16 with anti-PNR antibody was done (H), and number of PNR positive cells is

shown. Right graph are enlarged showing of values of rd1 and Cd9-KO;rd1 mice-derived retinas. (F, G) RT-qPCR to detect *Nr2e3* or *Rbo* was performed using total RNA obtained from whole retina at P10 or P16. Values are average of more than 3 samples from independent mice and expressed as relative to values of *Gapdh* and *Sdha* and average with standard deviation. The number of mice used in this experiment is; control at P10 (6), Cd9-KO at P10 (5), rd1 at P10 (6), Cd9-KO; rd1 at P10 (4), control at P16 (6), Cd9-KO at P16 (6) and Cd9-KO; rd1 at P16 (3). Statistical analysis was done by Tukey-Kramer method. (H, I) Immunohistochemical analysis of P16 and (I) P10 retinas derived from either from control, Cd9-KO, rd1, or Cd9-KO;rd1 mice. Frozen sections were immunostained with indicated antibodies. Nuclei were visualized by staining with DAPI (blue in H, gray in I). Scale bar: 50 μ m.

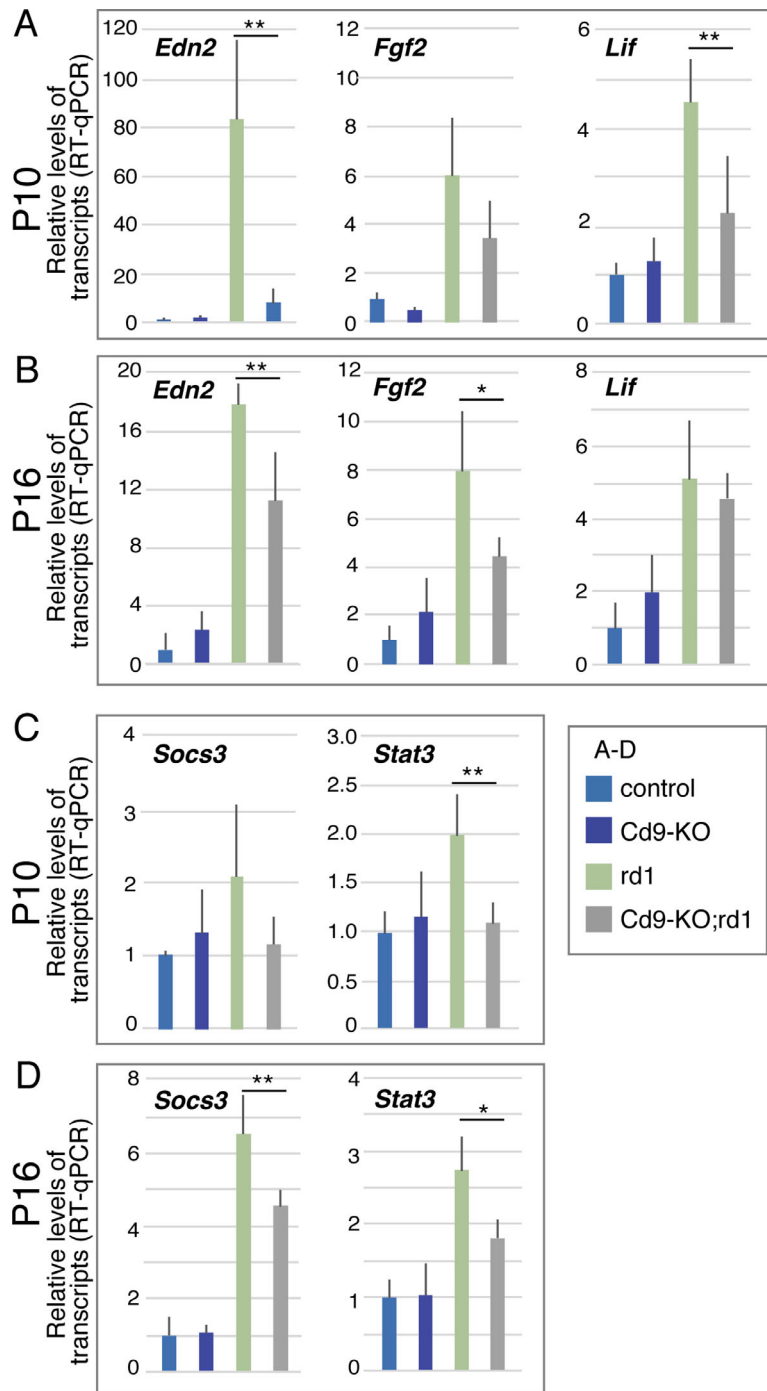


FIGURE 6. Induction of *Edn2* in degenerating photoreceptors was severely impaired in Cd9-KO;rd1 mouse retina. The retinas of control, Cd9-KO, rd1, or Cd9-KO;rd1 mice at (A, C) P10 or (B, D) P16 were isolated, and RT-qPCR was performed by using whole retina as templates. Values are average of more than 3 independent mice with standard deviation. The number of mice used in this experiment is; control at P10 (6), Cd9-KO at P10 (5), rd1 at P10 (6), Cd9-KO; rd1 at P10 (4), control at P16 (6), Cd9-KO at P16 (6) and Cd9-KO; rd1 at P16 (3). Statistical analysis was done by Tukey-Kramer method (* $P < 0.05$, ** $P < 0.01$).

was only slightly suppressed in retinas, suggesting that the lower level of *Edn2* was not caused by loss of *Lif* expression.

Signals of Il6st May Be Slightly Impaired in Cd9-KO;rd1 Retinas

We then focused on Il6st signals. Cd9 has been reported to stabilize Il6st protein in glioma stem cells, leading to STAT3 activation.³⁸ *Socs3* is one of genes that are activated by Il6st signaling, so we determined its expression in Cd9-KO;rd1 retinas. In P10 mouse retinas, the expression level of the *Socs3* transcript was comparable in the control, Cd9-KO, rd1, and Cd9-KO;rd1 mice (Fig. 6C). At P16, the expression level of the *Socs3* transcript in rd1 mice was increased, and the level was lower in Cd9-KO;rd1 mice-derived retinas when compared with rd1 retinas (Fig. 6D). The levels of Stat3 transcripts were lower in Cd9-KO;rd1 retinas at both P10 and P16 (Fig. 6D). Taken together, these results suggested that Il6st signals were inhibited in Cd9-KO;rd1 retinas when compared with rd1 retinas.

DISCUSSION

In the present study, we found a unique and cell type-specific dynamism of *Cd9* expression when photoreceptors were damaged. This phenomenon was thought to be commonly observed during the induction of photoreceptor degeneration. We therefore hypothesized an important biological function of Cd9 during photoreceptor injury. Our data strongly indicate that Cd9 has a protective function for photoreceptors in such emergencies. We found upregulation of *Edn2* transcripts, which may be one of the mechanisms in the protective role of Cd9 in photoreceptor degeneration.

Edn2 is a member of the endothelin family, which are vasoconstrictors. In contrast to *Edn1*, which has been well studied because it has potent effects on the vasculature,³⁹ limited knowledge is available on *Edn2*. *Edn2* transcripts are known to be highly expressed during retinopathy of prematurity and diabetic retinopathy.³⁹⁻⁴¹ The induction of *Edn2* transcripts has been reported in photoreceptors of diverse photoreceptor degeneration models.⁴² In addition, in the acute light damage model, expression of endothelin receptor B (*Ednrb*) transcripts is increased in Müller glia.⁴² Therefore, it has been suggested that *Edn2* produced in degenerating rod photoreceptors acts on Müller glia to protect the photoreceptors.³⁷ This possibility is also supported by intravitreal injection of an EDNRB antagonist (BQ-788), which results in increased photoreceptor loss in VPP mice, which have inherited photoreceptor degeneration.³⁶ In addition, intravitreal injection of BQ-3020, an endothelin receptor agonist, reduces photoreceptor apoptosis following retinal light damage.³⁶ In the current study, we showed strong suppression of induction of *Edn2* transcription in Cd9-KO;rd1 retinas at P10, therefore reduced level of *Edn2* expression may participate the severe phenotype of photoreceptor degeneration in Cd9-KO, but further work is necessary to evident this hypothesis.

Several studies have reported that LIF induces *Edn2* transcription in photoreceptor degeneration models.³⁶ In a similar manner to *Edn2*, lack of LIF resulted in accelerated photoreceptor degeneration with the loss of *Edn2* transcriptional activation.^{36,43} LIF is also upregulated in light-induced damaged retina⁴⁴ and several other retinal injury models.^{36,45} Induction of LIF is observed in a subset of Müller glia, and

in the absence of *Lif*, Müller glia remain quiescent.³⁶ We observed GFAP induction in Müller glia cells in Cd9-KO mice and the relatively normal induction level of LIF in the retinas of Cd9-KO mice. Based on these observations, we concluded that the level of *Lif* may not be a major cause of suppression of *Edn2* expression, leading us to examine downstream of the *Lif* receptor. In glioblastomas, Cd9 has been reported to stabilize Il6st, a common β subunit of the IL-6 and LIF receptors, by preventing ubiquitination-dependent lysosomal degradation.³⁸ In the absence of Cd9, the level of Il6st protein was markedly reduced in this model.³⁸

Edn2 expression in P10 retinas was severely suppressed in Cd9-KO;rd1 mice retinas; however, suppressions of *Lif*, *Socs3*, and *Stat3* were mild or not statistically significant. In addition, the level of *Edn2* expression in rd1 retinas decreased at P16, opposite the results for other genes examined. These results indicate that inhibited Il6st signals may only partially explain the suppression of *Edn2*. Furthermore, the results suggest a lower contribution of *Lif* in P10 retinas to the upregulation of *Edn2*. We hypothesize that the presence of *Lif*-dependent and -independent phases of *Edn2* transcriptional activation depend on the progression of degeneration. Because almost complete loss of *Edn2* upregulation in *Lif*-KO mice has been reported,^{36,43} analyses of changes in *Edn2* expression levels during the progression of photoreceptor degeneration may provide a way to test this hypothesis. In the case of rd1 mice, there was no independent mechanism from LIF signals; therefore, unknown mechanism(s) from Cd9 may contribute to enhanced upregulation of *Edn2* by LIF signaling during photoreceptor degeneration. To identify such a collaborative mechanism, enhanced analyses of *Edn2* are planned in future studies.

We initially focused on the high expression level of Cd9 in Müller glia. However, gross morphological development of Müller glia was not inhibited, and activation of Müller glia was the same as in control retinas when photoreceptors were damaged. In the case of MNU treatment, activation of Müller glia was more significant at day 3 after MNU administration, but we do not know whether the difference was caused by lack of Cd9 expression in Müller glia or by a more severe progression of photoreceptor degeneration. Furthermore, whether downregulation of Cd9 in Müller glia during photoreceptor degeneration has a biological significance, such as modifying cytokine secretion, is presently unknown.

We found that Cd63 was also upregulated in damaged photoreceptors (data not shown). Cd63 is expressed in endosomes,⁴⁶ this differs from Cd9, which is localized in the plasma membrane. However, both Cd63 and Cd9 are well-known molecules expressed in exosomes.⁴⁷ Although extensive studies have provided evidence of exosome secretion from the RPE, no similar results have been reported for the photoreceptors. Whether upregulation of Cd63 and of Cd9 contribute together in a positive or negative manner during the progression of degeneration via exosomes or formation of tetraspanin-enriched microdomains needs to be clarified in future studies.

Cd81 was also upregulated in degenerating photoreceptors (data not shown). Cd9 and Cd81 are expressed on the apical surface of RPE cell lines, and the roles of Cd81 in the particle-binding step of RPE phagocytosis through interaction with $\alpha V\beta 5$ integrin have been reported.⁴⁸ However, we found that gross morphological development, including photoreceptors of Cd9/Cd81-DKO retinas, was indistinguishable from that in the control. Impaired

phagocytosis of RPE causes photoreceptor degeneration in general,⁴⁹ but $\beta 5$ -deficient mice ($\beta 5$ -KO) showed normal gross retinal morphology, although $\beta 5$ -KO RPE lost phagocytic activity.⁵⁰ Although we have not examined photoreceptor degeneration in the Cd9/Cd81-DKO mice, it is possible that lack of Cd9 in the RPE also contributes to accelerated photoreceptor degeneration. Together with Cd9-KO, the Cd9/Cd81-DKO mouse model offers useful tools to analyze the roles of the molecular mechanism of photoreceptor degeneration involving different cell lineages in the eye.

Acknowledgments

The authors thank Asano Tshuko and Miho Nagoya for their excellent technical assistance.

Disclosure: **T. Iwagawa**, None; **Y. Aihara**, None; **D. Umotoni**, None; **Y. Baba**, None; **A. Murakami**, None; **K. Miyado**, None; **S. Watanabe**, None

References

- Miyake M, Koyama M, Seno M, Ikeyama S. Identification of the motility-related protein (MRP-a), recognized by monoclonal antibody M31-15, which inhibits cell motility. *J Exp Med*. 1991;174:1347–1354.
- Powner D, Kopp P, Monkley SJ, Critcheley DR, Berditchevski. Tetraspanin CD8 in cell migration. *Biochem Soc Trans*. 2011;39:563–567.
- Miyake M, Nakano K, Itoi SI, Koh T, Taki T. Motility-related protein-a (MRP-1/CD9) reduction as a factor of poor prognosis in breast cancers. *Cancer Res*. 1996;56:1244–1249.
- Helmler ME. Tetraspanin proteins promote multiple cancer stages. *Nat Rev Cancer*. 2014;14:49–60.
- Iwasaki T, Takeda Y, Maruyama K, et al. Deletion of tetraspanin CD9 diminishes lymphangiogenesis in vivo and in vitro. *J Biol Chem*. 2013;288:2118–2131.
- Stipp CS. Laminin-binding integrins and their tetraspanin partners as potential antimetastatic targets. *Expert Rev Mol Medicine*. 2010;12:e3.
- Helmler ME. Tetraspanin proteins mediate cellular penetration, invasion, and fusion events and define a novel type of membrane microdomain. *Annu Rev Cell Dev Biol*. 2003;19:397–422.
- Reyes R, Carderis B, Machado-Pineda Y, Cabanas C. Tetraspanin CD9: a key regulator of cell adhesion in the immune system. *Front Immunol*. 2018;9:863.
- Podergajs N, Motaln H, Rajcevic U, et al. Transmembrane protein CD9 is glioblastoma biomarker, relevant for maintenance of glioblastoma stem cells. *Oncotarget*. 2016;7:593–609.
- Wang GP, Han XF. CD9 modulates proliferation of human glioblastoma cells via epidermal growth factor receptor signaling. *Mol Med Rep*. 2015;12:1381–1386.
- Tole S, Patterson PH. Distribution of Cd9 in the developing and mature rat nervous system. *Dev Dyn*. 1993;197:94–106.
- Banerjee SA, Hadjiargyrou M, Patterson PH. An antibody to the tetraspan membrane protein CD9 promotes neurite formation in a partially $\alpha 3\beta 1$ integrin-dependent manner. *J Neurosci*. 1997;17:2756–2765.
- Martin-Alonso J-M, Hernando N, Bhosh S, Coca-Prados M. Molecular cloning of the bovine CD9 antigen from ocular ciliary epithelial cells. *J Biochem*. 1992;112:63–67.
- Klassen H, Ziaieian B, Kirov I, Young MJ, Schwartz PH. Isolation of retinal progenitor cells from post-mortem human tissue and comparison with autologous brain progenitors. *J Neurosci Res*. 2004;77:334–343.
- Mochizuki Y, Iida A, Lyons E, et al. Use of cell type-specific transcriptome to identify genes specifically involved in Müller glia differentiation during retinal development. *Dev Neurobiol*. 2014;74:426–437.
- Miyado K, Yamada G, Yamada S, et al. Requirement of CD9 on the egg plasma membrane for fertilization. *Science*. 2000;287:321–324.
- Takeda Y, He P, Tachibana I, et al. Double deficiency of tetraspanins CD9 and CD81 alters cell motility and protease production of macrophages and causes chronic obstructive pulmonary disease-like phenotype in mice. *J Biol Chem*. 2008;283:26089–26097.
- Iida A, Iwagawa T, Kuribayashi H, et al. Histone demethylase Jmjd3 is required for the development of subsets of retinal bipolar cells. *Proc Natl Acad Sci USA*. 2014;111:3751–3756.
- Iida A, Shinoe T, Baba Y, Mano H, Watanabe S. Dicer plays essential roles for retinal development by regulation of survival and differentiation. *Invest Ophthalmol Vis Sci*. 2011;52:3008–3017.
- Terada N, Baracska K, Kinter M, et al. The tetraspanin protein, CD9, is expressed by progenitor cells committed to oligodendrogenesis and is linked to beta1 integrin, CD81, and Tspan-2. *Glia*. 2002;40:350–359.
- Ueno K, Iwagawa T, Kuribayashi H, et al. Transition of differential histone H3 methylation in photoreceptors and other retinal cells during retinal differentiation. *Sci Rep*. 2016;6:29264.
- Ohtsuka T, Imayoshi I, Shimojo H, Nishi E, Kageyama R, McConnell SK. Visualization of embryonic neural stem cells using Hes promoters in transgenic mice. *Mol Cell Neurosci*. 2006;31:109–122.
- Ueno K, Iwagawa T, Ochiai G, et al. Analysis of Muller glia specific genes and their histone modification using Hes1-promoter driven EGFP expressing mouse. *Sci Rep*. 2017;7:3578.
- Wright MD, Tomlinson MG. The ins and outs of the transmembrane 4 superfamily. *Immunology Today*. 1994;15:588–594.
- Rubinstein E, Ziyat A, Prenant M, et al. Reduced fertility of female mice lacking CD81. *Dev Biol*. 2006;290:351–358.
- Charrin S, Latil M, Soave S, et al. Normal muscle regeneration requires tight control of muscle cell fusion by tetraspanins CD9 and CD81. *Nat Commun*. 2013;4:1–12.
- Martin F, Roth DM, Jans DA, et al. Tetraspanins in viral infections: a fundamental role in viral biology? *J Virology*. 2005;79:10839–10851.
- Takeda Y, Tachibana I, Miyado K, et al. Tetraspanins CD9 and CD81 function to prevent the fusion of mononuclear phagocytes. *J Cell Biol*. 2003;161:945–956.
- Vazquez-Chona F, Song BK, Geisler EE, Jr. Temporal changes in gene expression after injury in the rat retina. *Invest Ophthalmol Vis Sci*. 2004;45:2737–2746.
- Nambu H, Yuge K, Nakajima M, et al. Morphologic characteristics of N-methyl-N-nitrosourea-induced retinal degeneration in C57BL mice. *Pathol Int*. 1997;47:377–383.
- Herrold KM. Pigmentary degeneration of the retina induced by N-Methyl-N-Nitrosourea. *Arch Ophthalmol*. 1967;78:650–653.
- Nilsson SE, Knave B, Ersson HE. Changes in ultrastructure and function of the sheep pigment epithelium and retina induced by sodium iodate. II. Early effects. *Acta Ophthalmol*. 1977;55:1007–1266.
- Enzmann V, Row BW, Yamauchi Y, et al. Behavioral and anatomical abnormalities in a sodium iodate-induced model

- of retinal pigment epithelium degeneration. *Exp Eye Res.* 2006;82:441–448.
34. Carter-Dawson LD, LaVail MM, Sidman RL. Differential effect of the rd mutation on rods and cones in the mouse retina. *Invest Ophthalmol Vis Sci.* 1978;17:489–498.
 35. Kobayashi M, Takezawa S-I, Hara K, et al. Identification of a photoreceptor cell-specific nuclear receptor. *PNAS.* 1999;96:4814–4819.
 36. Joly S, Lange C, Thiersch M, Samardzija M, Grimm C. Leukemia inhibitory factor extends the lifespan of injured photoreceptors in vivo. *J Neurosci.* 2008;28:13765–13774.
 37. Bramall AN, Szego MJ, Pacione LR, et al. Endothelin-2-mediated protection of mutant photoreceptors in inherited photoreceptor degeneration. *PlosOne.* 2013;8:e58023.
 38. Shi Y, Zhou W, Cheng L, et al. Tetraspanin CD9 stabilizes gp130 by preventing its ubiquitin-dependent lysosomal degradation to promote STAT3 activation in glioma stem cells. *Cell Death Diff.* 2017;24:167–180.
 39. Alrashdi SF, Deliyanti D, Talia DM, Wilkinson-Berka JL. Endothelin-s injures the blood-retinal barrier and macroglial Muller cells. *American J Pathol.* 2018;188:805–816.
 40. Binz N, Rakoczy EP, Ali Rahman IS, Vagaja NN, Lai C-M. Biomarkers for diabetic retinopathy-could endothelin 2 be part of the answer? *PlosOne.* 2016;11:e0160442.
 41. Paterl C, Narayanan SP, Zhang W, et al. Activation of the endothelin system mediates pathological angiogenesis during ischemic retinopathy. *Am J Pathol.* 2014;184:3040–3051.
 42. Rattner A, Nathans J. The genomic response to retinal disease and injury: evidence for endothelin signaling from photoreceptors to glia. *J Neurosci.* 2005;25:4540–4549.
 43. Burgi S, Samardzija M, Grimm C. Endogenous leukemia inhibitory factor protects photoreceptor cells against light-induced degeneration. *Mol Vis.* 2009;15:1631–1637.
 44. Smardzija M, Wenzel A, Auenberg S, Thiersch M, Reme C, Grimm C. Differential role of Jak-STAT signaling in retinal degenerations. *FASEB J.* 2006;20:2411–2413.
 45. Naash MI, Hollyfield JG, Al-Ubaidi MR, Baehr W. Stimulation of human autosomal dominant retinitis pigmentosa in transgenic mice expressing a mutated murine opsin gene. *Proc Natl Acad Sci.* 1993;90:5499–5503.
 46. Pols M, Klumperman J. Trafficking and function of the tetraspanin CD63. *Exp Cell Res.* 2009;315:1584–1592.
 47. Reyes R, Cardenes B, Machado-Pineda Y, Cabanas C. Tetraspanin CD9: a key regulator of cell adhesion in the immune system. *Front Immunol.* 2018;9:863.
 48. Chang Y, Finnemann SC. *J Cell Sci.* 2007;120:3053–3063.
 49. Nandrot EF. Animal models, in “The quest to decipher RPE phagocytosis”. *Adv Exp Med Biol.* 2014;801:77–83.
 50. Nandrot EF, Kim Y, Brodies SE, Huang X, Sheppard D, Finnemann SC. Loss of synchronized retinal phagocytosis and age-related blindness in mice lacking alphavbeta5 integrin. *J Exp Med.* 2004;200:1539–1545.